JOURNAL OF SOLID STATE CHEMISTRY 56, 1–11 (1985)

Phase Equilibria in the Ce–O and Ce–Fe–O Systems

KENZO KITAYAMA, KIYOSHI NOJIRI,* TADASHI SUGIHARA,† AND TAKASHI KATSURA

Department of Chemistry, Faculty of Science, Tokyo Institute of Technology, Ookayama, Meguro-ku, Tokyo 152, Japan

Received February 8, 1984; in revised form June 4, 1984

Phase equilibria in the Ce–O system at 1000, 1100, 1153, 1200, 1249, 1310, and 1330°C and those in the Ce–Fe–O system at 1000, 1100, and 1200°C were established. The former system has CeO_2 with a fluorite type, Ce_3O_5 with a C-type rare-earth oxide, and Ce_2O_3 with a A-type rare-earth oxide. CeO_2 and Ce_3O_5 have nonstoichiometric compositions, but the stoichiometry of Ce_2O_3 was confirmed at 1200, 1249, and 1310°C. In the latter system, only the one ternary compound $CeFeO_3$ was confirmed under present experimental conditions. On the basis of the established phase diagrams, the standard Gibbs energies of the reactions: (1) $\frac{3}{2}\,Ce_2O_3 + \frac{1}{4}\,O_2 = Ce_3O_5$, (2) $\frac{1}{3}\,Ce_3O_5 + \frac{1}{6}\,O_2 = CeO_2$, (3) $\frac{1}{3}\,Fe_3O_4 + CeO_2 = CeFeO_3 + \frac{1}{6}\,O_2$, and (4) $Fe + CeO_2 + \frac{1}{2}\,O_2 = CeFeO_3$, were determined at various temperatures. Also relationships between $\Delta G°$ and the temperatures of the same reactions were determined within the experimental temperature range.

Many reports (*1–9*), have been published for the Ce − O system, especially about Ce_2O_3–CeO_2. Bevan (*1*) presented the ordered intermediate phases in the CeO_2–Ce_2O_3 and indicated the formation of a number of ordered phases; $Ce_{32}O_{58}$, $Ce_{32}O_{57}$, and $Ce_{18}O_{31}$ having a rhombohedral structure, and a phase having the C-type rare-earth structure with a composition range extending between the approximate $Ce_{32}O_{53}$ and $Ce_{32}O_{54}$. Also he reported that the solid solution range of the CeO_2-phase was narrow, and that the A-type rare-earth Ce_2O_3-phase appears to have a solid solution range between $CeO_{1.50}$ and $CeO_{1.53}$. Systematic measurements of the oxygen dissociation pressure in the system of the cerium oxides from CeO_2 to Ce_2O_3 were reported in the temperature ranges from 600 to 1050°C by Brauer *et al.* (*2*) using a dynamic method with appropriate hydrogen–water-vapor mixtures. In addition, samples of cerium oxides with the composition from $CeO_{2.00}$ to $CeO_{1.78}$ were examined by the high-temperature X-ray diffraction method between 20 and 1000°C by Brauer and Gingerich (*3*). From these experiments the phase relationship in this region was fully explained for the first time; a homogenous series of mixed crystals with the cubic fluorite structure exists at a higher temperature than 685°C, as had been predicted for the system. Kuznetsov *et al.* (*4*) reported on the oxygen dissociation pressures in the Ce_2O_3-CeO_2 system for the temperature range from 694 to 1014°C, by using

* Present address: Saitama Institute of Environmental Pollution, 639-1 Kamiokubo, Urawa, Saitama 338.

† Present address: Mitsubishi Metal Research Institute, 1-297 Kitabukuro, Omiya, Saitama 330.

0022-4596/85 $3.00

emf measurements; and they established the phase relationships for these oxides.

Thermodynamic studies for $CeO_{1.5}$ to CeO_2 and the nonstoichiometric cerium oxide were performed by Bevan and Kordis (*5*), Compserveux and Gerdanian (*6*), Panlener *et al.* (*7*), and Iwasaki and Katsura (*8*). Bevan and Kordis (*5*) have determined the oxygen pressures in equilibrium with the cerium oxides by the equilibration with CO/CO_2 or H_2/H_2O mixtures in the temperature range from 636 to 1169°C, and partial and integral free energies, enthalpies, and entropies have been calculated. They also constructed the cerium–oxygen phase diagram at these temperatures between the compositions $CeO_{1.5}$ and $CeO_{2.0}$. According to calorimetric measurements (*6*) of the partial molar enthalpy of solution of O_2 in cerium oxides at 1353 K, a two-phase area appears in the region r = 1.50–1.65, a one-phase area in the region r = 1.65–1.70, a two-phase area in the region r = 1.70–1.72, and a one-phase area in the region r = 1.72–2.00. Here, r is oxygen to metal ratio, O/Ce. Panlener *et al.* (*7*) reported that the ordered phases observed by Bevan and Kordis between $CeO_{1.72}$ and $CeO_{1.70}$ have not been observed in their study at temperatures between 1300 and 1500°C. Iwasaki and Katsura (*8*) investigated the thermodynamic properties of the nonstoichiometric ceric oxides at temperatures ranging from 900 to 1300°C, using a thermobalance and calculated the activities of Ce_2O_3 and CeO_2 in the solid solutions, and relative partial enthalpies and entropies of the Ce_2O_3 and CeO_2. Partial molar thermodynamic quantities for oxygen in nonstoichiometric cerium oxides were also determined by thermogravimetric analysis in CO/CO_2 mixtures in the temperature range 900–1400°C (*9*). The results showed that the α'-phase in the phase diagram, previously described as a grossly nonstoichiometric phase, can be divided into several subregions each consisting of an apparent nonstoichiometric single phase.

In view of the uncertainty on this system arising from these results in the literature, further investigations seemed desirable and the present experiment will present additional data.

Phase equilibria in the $Fe–Fe_2O_3–Ln_2O_3$ system has been established at 1200°C by us (*10–16*). It has been elucidated that these systems could be classified into four groups with respect to the assemblage of the ternary compounds. According to this proposal, the $Fe–Fe_2O_3–(La$ and $Nd)_2O_3$ systems belong to the A-type in which only one ternary compound $LnFeO_3$ is stable, the $Fe–Fe_2O_3–(Sm$, Eu, Gd, Tb, and $Dy)_2O_3$ systems belong to the B-type with two ternary compounds, $LnFeO_3$ and $Ln_3Fe_5O_{12}$, the $Fe–Fe_2O_3–(Ho$, Er, and $Tm)_2O_3$ systems belong to the C-type with three ternary compounds, $LnFeO_3$, $Ln_3Fe_5O_{12}$, and $LnFe_2O_4$, while the $Fe–Fe_2O_3–(Yb$ and $Lu)_2O_3$ systems belong to the D-type with four compounds, $LnFeO_3$, $Ln_3Fe_5O_{12}$, $LnFe_2O_4$, and $Ln_2Fe_3O_7$. Tannieres (*17*) also investigated the phase equilibria in $Fe–Fe_2O_3–(Tm$, Yb, and $Lu)_2O_3$ over the temperature range 900–1200°C. The system with cerium oxide can be expected to form another type of phase diagram because of the various types of oxides; that is, CeO_2 is a typical fluorite type oxides, the tetravalent Ce_2O_3 (*1*) is of the rare-earth C-type oxide structure, and the trivalent Ce_2O_3 is of the rare-earth A-type oxide structure.

Only one ternary compound $CeFeO_3$ with a perovskite structure has been found in the reports (*18, 19*) in the Fe–Ce–O system. On the contrary, Tretyakov *et al.* (*20*) reported that a compound $Ce_2Fe_2O_7$ with a pyrochlore structure is formed upon heating a mixture of hematite and cerium dioxide, containing 40–70% of the latter in the air. Recently Tretyakov *et al.* (*20*) investigated the phase equilibria and the thermodynamics of coexisting phases in the Ce–

Fe–O system at 1300 K, and showed that only the ternary compound $CeFeO_3$ with the perovskite structure occurs.

The purpose of the present investigations are: (1) to establish the precise phase equilibria in the Ce–O and Ce–Fe–O systems in the temperature ranges 1000 to 1330°C for the former system and at 1000, 1100, and 1200°C for the latter system by changing the oxygen partial pressure, and (2), to determine the standard Gibbs energies of the reactions at each temperature which are shown in the established phase diagrams.

Experimental

Analytical grade of Fe_2O_3 (99.9%) and CeO_2 (99.9%), which were dried at 1000°C overnight, were used as the starting materials. The desired ratios of CeO_2 to Fe_2O_3 were obtained by mixing thoroughly in an agate motar under ethyl alcohol. The mixtures thus obtained and CeO_2 in the case of Ce–O system were treated by the procedures described in the previous report (*10*). The apparatus and procedures for controlling the oxygen partial pressures and keeping a constant temperature, the method of thermogravimetry, the method of the actual oxygen partial pressure measurement, and the method of chemical analysis are the same as those reported in the previous papers (*12, 13, 26–29*). Gas mixtures of CO_2 and CO were used in the temperature range lower than 1150°C; gas mixtures of CO_2 and O_2 were used in oxygen partial pressure range higher than 10^{-4} atm (1 atm = 1.013 × 10^5 Pa). In Fig. 1 the relationship between the calculated oxygen partial pressure (*23*) and the oxygen partial pressure measured by the CaO-stabilized ZrO_2 cell at 1000°C is shown as an example. Both values are in good agreement.

One atmosphere oxygen pressure was chosen as the reference state; the sample weight at the oxygen partial pressure of 1 atm was chosen as the reference weight throughout the present experiment.

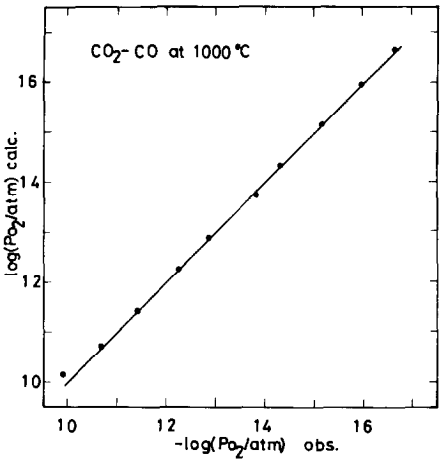

FIG. 1. The relationship between the calculated oxygen partial pressure and the oxygen partial pressure measured by CaO-stabilized ZrO_2 cell at 1000°C.

Results and Discussions

(*1*) *Phase Equilibria*

(*a*) *The Ce–O system.* To check the system of the apparatus used, the Fe–Fe_2O_3 system was first checked with the same procedures and apparatus. The results obtained were in good agreement with those of Darken and Gurry (*21, 22*) and Smiltens (*23*).

Before the study of Ce–Fe–O system was started, the Ce–O system was investigated at 1000, 1100, 1153, 1200, 1249, 1310, and 1330°C. The relationships between $-\log P_{O_2}$ and the composition of cerium oxide are shown in Fig. 2a at temperatures 1000, 1100, and 1200°C, together with some previous data. Here, the composition of oxide was indicated with x in CeO_x in ordinate. The present values are in good agreement with those of Panlener *et al.* (*7*) and Iwasaki and Katsura (*8*) except for two points in the latter at 1000°C. The results at temperatures 1153, 1200, 1249, 1310, and 1330°C in the range of $1.8 \geqq x \geqq 1.5$ are

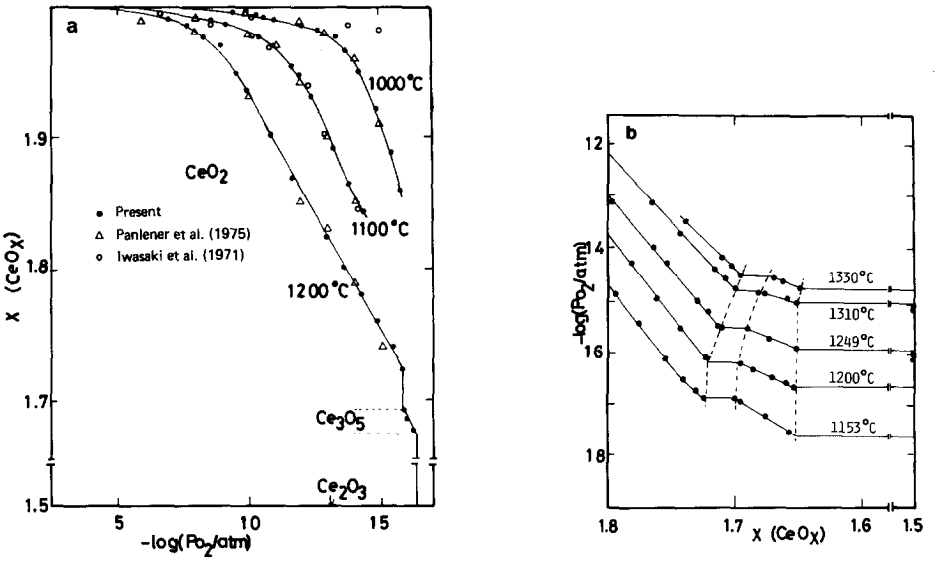

FIG. 2. The relationship between the oxygen partial pressure and the composition of cerium oxide. (a) 1000, 1100, and 1200°C; (b) 1153, 1200, 1249, 1310, and 1330°C.

shown separately in Fig. 2b to avoid confusion. From the thermogravimetric results, the results of the phase identification by the quench method, and the information from the literature described above, CeO_2 with the fluorite type, Ce_3O_5 with the rare-earth C-type oxide, and Ce_2O_3 with the rare-earth A-type oxide were found to be stable under the present experimental conditions. Both CeO_2 and Ce_2O_3 phases were easily confirmed by X-ray powder diffractometer using the quenched samples, but Ce_3O_5 had not been confirmed because of the instability of the phase. We attempted to synthesize Ce_3O_5 in $\log P_{O_2} = -16.50$ at 1200°C by the quench method but the quenched samples usually burned on the weighing paper and oxidized to CeO_2 in air as soon as the samples had been pulled out from the bottom of the furnace. According to Bevan (*1*) and Bevan and Kordis (*5*), Ce_3O_5 should be the rare-earth C-type oxide although they called it tetravalent Ce_2O_3 as described above. Sørensen (*9*) found the monoclinic phase, being isostructural with Pr_6O_{11}, in the system by high-temperature X-ray diffraction studies, at high temperatures between 790 and 855°C. Unfortunately, high-temperature X-ray apparatus was not available to us. The patterns of quenched samples of present studies in $\log P_{O_2} = -10.00$ to -15.00 usually were those of CeO_2 and of other compounds. The peaks of the other compound shifted to the lower angle side relative to those of CeO_2 and these seemed to be satellite peaks of CeO_2. Besides, 2θ values of CeO_2 (Table III) and of the other seemed not to change with P_{O_2}. The shifted peaks may have originated from CeO_x with monoclinic structure; but, the X-ray powder pattern of CeO_2, being originally similar to that of Pr_6O_{11}, made it difficult to identify these peaks. Hence, we could not confirm the new phase by the quench method. We theorize that 2θ values of CeO_2 at lower oxygen partial pressures may be shifted to lower 2θ values but this is not quenchable; the phase seems subdivided into two phases as if the ex-solution had occurred. The above inference would be supported by thermogravimetric data if no abrupt weight change would be found

under the present experimental conditions and techniques.

As is shown in Fig. 2, for example, at 1200°C, the CeO_2 phase with a composition $CeO_{1.72}$ is in equilibrium with Ce_3O_5 with a composition $CeO_{1.70}(Ce_3O_{5.10})$ having an equilibrium oxygen partial pressure −16.27 atm in log P_{O_2}. With further reduction, the Ce_3O_5 phase changes composition with oxygen partial pressure to $CeO_{1.65}(Ce_3O_{4.95})$; lastly, the phase changes to Ce_2O_3 phase at −16.70 atm. Under the present experimental conditions, Ce_2O_3 is stoichiometric above 1200°C as was confirmed by Bevan and Kordis (*5*) in the temperature range below 1150°C. In the one-phase areas of CeO_2 and Ce_3O_5, the weight decreases while decreasing the oxygen partial pressure, and these weight changes are reversible. This means the oxygen sublattices of these two might be defective in the nonstoichiometric oxides, as has been confirmed by means of the X-ray diffraction method by Faber *et al.* (*30*) for ceria.

In Table I the compositions of compounds, the stability ranges of the compounds in terms of log P_{O_2}, the symbols of the compounds, and the activities of the components in the solid solutions are tabulated at each temperature. Activities of the components in the solid solutions were calculated with Gibbs–Duhem equation using the thermogravimetric results of N_O/N_Y vs log P_{O_2} relation. Here, N_O and N_Y are the mole fraction of oxygen and the component Y. The relationship between the composition of Ce_3O_5 and log P_{O_2} was represented by a linear equation, $N_O/N_{Ce_3O_5} = a \log P_{O_2} + b$, from the thermogravimetric results. The constants a and b at various temperatures are shown in Table II. The method of the calculation of the activity will be shown in brief considering CeO_2 solid solution as an example. Taking the oxygen atom and CeO_2 as the component in this case, the Gibbs–Duhem equation is represented as

$$\log a_{CeO_2} = -\tfrac{1}{2}\int_{\log P_{O_2}(I)}^{\log P_{O_2}(II)} (N_O/N_{CeO_2})\, d \log P_{O_2}$$
$$= \tfrac{1}{2}\int_{\log P_{O_2}(x=2)}^{\log P_{O_2}(II)} (2 - x) d \log P_{O_2}.$$

Log $P_{O_2}(x = 2)$ was taken as the standard state; that is, the activity of CeO_2 at $x = 2$ was chosen as unity. In order to calculate the activity of CeO_2 of the composition F_3 at 1200°C, for example, log $P_{O_2} = -2.7$ and −16.27 were used as log $P_{O_2}(x = 2)$ and log P_{O_2}(II), respectively. In the case of the CeO_2 solid solution, the integration was carried out graphically.

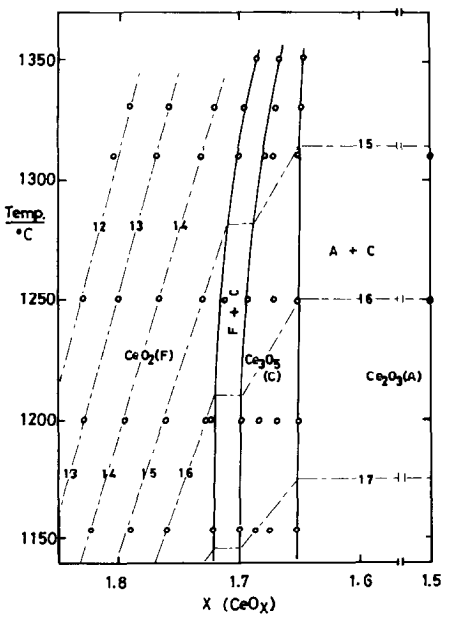

FIG. 3. The phase diagram of Ce_2O_3–CeO_2 system.

The Ce_2O_3–CeO_2 phase diagram under the present experimental conditions is shown in Fig. 3. The abscissa in the composition of cerium oxide was represented by x in CeO_x. The dotted line in the figure indicate the iso-oxygen partial pressure line and figures on the lines represent the oxygen partial pressure in $-\log P_{O_2}$. The symbols, F, C, and A indicate the same meanings as those in Table I. The outstanding features are that two-phase areas, F + C and A + C, do not change their width of

TABLE I

COMPOUNDS: ITS COMPOSITIONS, SYMBOLS, STABILITY RANGES IN OXYGEN PARTIAL PRESSURES, AND ACTIVITIES OF COMPONENTS IN THE SOLID SOLUTIONS

Temp. (°C)	Component	Composition	Symbol	log P_{O_2} (atm)	log a_i
1000	CeO_2	$CeO_{2.00}$	F	0–~4.0[a]	0
		$CeO_{1.99}$	F_1	10.72	0.010
		$CeO_{1.87}$	F_2	15.68	0.101
	Ce_2O_3	$Ce_2O_{3.00}$	R		0
	$CeFeO_3$	$CeFeO_{3.00}$	P	10.72–15.68	0
1100	CeO_2	$CeO_{2.00}$	F	0–~3.2[a]	0
		$CeO_{1.99}$	F_1	8.63	0.013
		$CeO_{1.86}$	F_2	13.96	0.162
	Ce_2O_3	$Ce_2O_{3.00}$	R		0
	$CeFeO_3$	$CeFeO_{3.00}$	P	8.63–13.96	0
1153	CeO_2	$CeO_{2.00}$	F	0–~3.0[a]	0
		$CeO_{1.72}$	F_3	16.91	0.563
	Ce_3O_5	$Ce_3O_{5.10}$	C_1	16.91	−0.0108
		$Ce_3O_{4.96}$	C	17.65	0
	Ce_2O_3	$Ce_2O_{3.00}$	R	17.65–	0
1200	CeO_2	$CeO_{2.00}$	F	0–~2.7[a]	0
		$CeO_{1.99}$	F_1	7.25	0.0134
		$CeO_{1.84}$	F_2	12.48	0.191
		$CeO_{1.72}$	F_3	16.27	0.600
	Ce_3O_5	$Ce_3O_{5.09}$	C_1	16.27	−0.0054
		$Ce_3O_{4.96}$	C	16.70	0
	Ce_2O_3	$Ce_2O_{3.00}$	R	16.70–	0
	$CeFeO_3$	$CeFeO_{3.00}$	P	7.25–12.48	0
1249	CeO_2	$CeO_{2.00}$	F	0–~2.5[a]	0
		$CeO_{1.71}$	F_3	15.55	0.637
	Ce_3O_5	$Ce_3O_{5.07}$	C_1	15.55	0.0029
		$Ce_3O_{4.95}$	C	16.00	0
	Ce_2O_3	$Ce_2O_{3.00}$	R	16.00–	0
1310	CeO_2	$CeO_{2.00}$	F	0–~2.5[a]	0
		$CeO_{1.70}$	F_3	14.87	0.654
	Ce_3O_5	$Ce_3O_{5.05}$	C_1	14.87	−0.0002
		$Ce_3O_{4.95}$	C	15.10	0
	Ce_2O_3	$Ce_2O_{3.00}$	R	15.10–	0
1330	CeO_2	$CeO_{2.00}$	F	0–~2.3[a]	0
		$CeO_{1.69}$	F_3	14.57	0.703
	Ce_3O_5	$Ce_3O_{5.00}$	C_1	14.57	−0.00234
		$Ce_3O_{4.94}$	C	14.83	0
	Ce_2O_3	$Ce_2O_{3.00}$	R	14.83–	0

[a] These values were obtained by means of the extrapolation using the results of the thermogravimetry.

TABLE II

THE CONSTANTS a AND b IN THE EQUATION OF $N_O/N_Y = a \log P_{O_2} + b$ OF THE Ce_3O_5 SOLID SOLUTION AT VARIOUS TEMPERATURES

°C	a	b
1153	0.191	3.32
1200	0.321	5.32
1249	0.267	4.22
1310	0.417	6.25
1330	0.312	4.56

composition with the change in temperature; on the other hand, the width of one-phase area of C become narrower with the temperature increase as if it could compensate the increase of the width of the F phase.

(*b*) *The Ce–Fe–O system.* Fe_2O_3 and CeO_2 are stable in the atmosphere of 1 atm oxygen. Five samples with $CeO_2/FeO_{1.5}$ mole ratios 3/1, 65/35, 1, 1/2, and 1/4 were prepared for use in the thermogravimetric experiments. The thermogravimetric results of the two samples, 65/35 and 1/2, are shown in Fig. 4 as representative of the set. In the figures the abscissa represents the oxygen partial pressure in log P_{O_2} in atmospheres and the ordinate R indicates the mole ratio of oxygen to metal, $n_O/(n_{Ce} + n_{Fe})$. Here, n_O, n_{Ce}, and n_{Fe} mean the mole number of the respective elements represented by the subscripts.

The identification of the phases was performed with quenched samples by using the powder X-ray diffractometer with Fe$K\alpha$ radiation. The following phase combinations were found: $CeO_2 + Fe_2O_3$, $CeO_2 + Fe_3O_4$, $CeO_2 + CeFeO_3$, $CeO_2 + \alpha$-Fe, $CeFeO_3 + Fe_3O_4$, $CeFeO_3$ + "FeO," and $CeFeO_3 + \alpha$-Fe.

Based upon the results of the thermogravimetry and the identification of the phases, a phase diagram with apices Ce_2O_3, Fe, and oxygen was drawn and its diagram at 1200°C is shown in Fig. 5 as representative. Figures in the three-phase areas in Fig. 5 are the equilibrium oxygen partial pressure in $-\log P_{O_2}$. As can be observed in Fig. 5, only one ternary compound Ce FeO_3(P) is stable under the present conditions. It is very easy to explain Fig. 5: If the

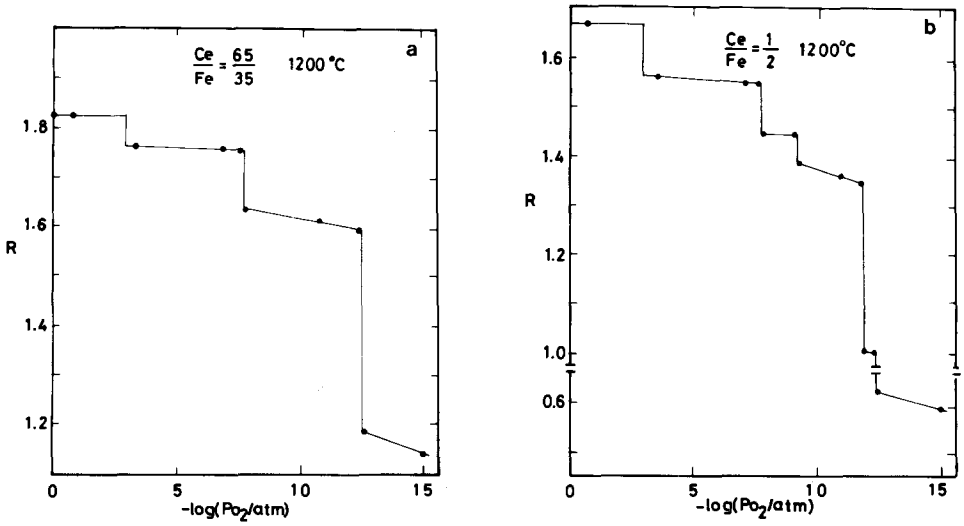

FIG. 4. The relationship between log P_{O_2} and the composition at 1200°C. (a) Ce/Fe = 65/35, (b) Ce/Fe = 1/2.

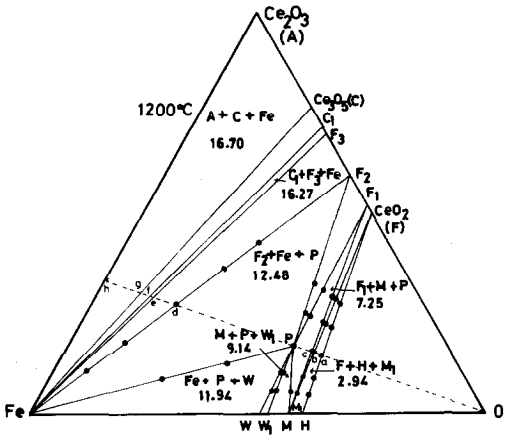

FIG. 5. The phase equilibia in the Ce_2O_3–Fe–O system at 1200°C. Numerical values in the three solid phases regions are the equilibrium oxygen partial pressure in $-\log P_{O_2}$. Symbols are the same as those in Table I.

mixture of composition *a* were reduced, the composition would change along the dotted line originated from apex 0. The mixture of CeO_2 and Fe_2O_3 with the composition *a* is stable in the oxygen partial pressure from zero to −2.94 atm in $\log P_{O_2}$. In the P_{O_2} range $\log P_{O_2} < -2.94$, the composition *a* changes to the composition *b* with two phases, $Fe_3O_4(M_1)$ + $CeO_2(F)$, on decomposing Fe_2O_3 to Fe_3O_4. In the oxygen partial pressure between −2.94 and −7.25 in $\log P_{O_2}$, the total composition changes from *b* to *c* with changing cerium oxide composition from F to F_1 and the iron oxide composition from M_1 to M. In the oxygen partial pressure range $\log P_{O_2} < -7.25$, the total composition reaches $CeFeO_3(P)$ from *c*. $CeFeO_3$ is stable in the oxygen partial pressure from 7.25 to 12.48 in $-\log P_{O_2}$. At $\log P_{O_2} = -7.25$ three phases, $CeFeO_3$ + $Fe_3O_4(M)$ + Ce-oxide(F_1) and at $\log P_{O_2} = -12.48$ three phases, $CeFeO_3$ + α-Fe + Ce-oxide(F_2), coexist in equilibrium. After the total composition reached *d*, the weight decreases to *e* with a change in cerium oxide composition from F_2 to F_3 and while keeping α-Fe composition constant. At this point three-phase area, F_3 + C_1 + α-Fe, appears in equilibrium with the oxygen partial pressure $\log P_{O_2} = -16.27$. In the oxygen partial pressure between −16.27 and −16.70 in $\log P_{O_2}$, a two-phase region appears, the composition of α-Fe being constant and that of Ce_3O_5 changing from C_1 to C. At this juncture the total composition changes from *g* to *h*, which is a two-phase area, α-Fe + Ce_2O_3, in the oxygen partial pressure less than $\log P_{O_2} = -16.70$.

The phase diagrams at 1000 and 1100°C showed the same pattern as that of 1200°C. The compositions of each compound and activities of each component are shown in Table I, together with those of 1200°C.

As the previous reports have shown, the other lanthanoid perovskites are stable in the air, but $CeFeO_3$ is unstable in the air as described above.

$CeFeO_3$ seems to have a slightly nonstoichiometric compositions in the temperature range from 1000 to 1200°C, as has already been pointed out by Tretyakov *et al.* (*20*). The composition is $CeFeO_{2.97}$ at 1000°C, $CeFeO_{2.98}$ at 1100°C, and $CeFeO_{2.99}$ at 1200°C by thermogravimetry.

The present phase diagram pattern in a sense belongs to A-type on account of the presence of one ternary compound, but strictly speaking, it does not belong to the A-type as $CeFeO_3$ is unstable in the air.

The equilibrium phase diagram of Ce–Fe–O system at 1300 K has been reported by Tretyakov *et al.* (*20*). The difference in the pattern between the present one and Tretyakov's has arisen in the three- and two-phase regions. The regions VIII and X called by Tretyakov *et al.* have three phases, CeO_2 + Fe_3O_4 + $CeFeO_3$ and CeO_2 + CeO_{2-x} + $CeFeO_3$, respectively. As is shown in Fig. 5, the present diagram also has a three-phase region of Ce-oxide(F_1) + Fe_3O_4 + $CeFeO_3$. But Ce-oxide(F_1) is nonstoichiometric in the present case. There is no such three-phase region in the present results as region X in the Tretyakov's. Ac-

cording to the present results of the Ce–O system, the CeO_2 phase has the wide range of solid solution. So it must be a two-phase region, CeO_2 solid solution + $CeFeO_3$, in which CeO_2 solid solution varies its composition from F_1 to F_2 changing with the oxygen partial pressure. There are other two-phase regions: the Fe_3O_4 solid solution (M_1 to M) + CeO_2 solid solution (F to F_1), and the α-Fe + CeO_2 solid solution (F_2 to F_3), in the present phase diagram which was not found in the diagram of Tretyakov *et al.* These discrepancies principally resulted from the Ce-oxide solid solution range.

The measured unit-cell parameters of the compounds, CeO_2, Fe_2O_3, Fe_3O_4, and $CeFeO_3$ are shown in Table III, together with the values in the previous reports. Compounds in the third column are the coexisting phases with the oxides listed in the first column. Values obtained are in good agreement with each other. It seems to be that the coexisting phases do not affect the lattice parameters of these oxides, and that CeO_2, Fe_2O_3, and Fe_3O_4 might be stoichiometric toward the Fe_2O_3, CeO_2, and CeO_2 side, respectively. The lattice parameters of $CeFeO_3$ are not affected by the oxygen partial pressure.

(2) *Calculation of the Standard Gibbs Energies of Reaction*

On the basis of the established phase diagrams, the standard Gibbs energies of reactions can be calculated by an equation $\Delta G^\circ = -RT \ln K$. Here, the R is the gas constant, the T the absolute temperature, and the K the equilibrium constant of each reaction. Activities of the components in the solid solutions which are necessary for the calculation are tabulated in Table I. The activity of the CeO_2 component at the composition F, that of Ce_3O_5 the component at the composition C, that of the Ce_2O_3 component at the composition R, and that of the $CeFeO_3$ at the composition P are chosen as unity in the present report, as is shown in Table I. The reactions in the present phase diagrams, the equilibrium oxygen partial pressures, and the ΔG° values obtained are shown in Table IV. As for the equilibrium oxygen partial pressure of the reaction (3)

TABLE III

UNIT CELL DIMENSIONS OF THE COMPOUNDS PREPARED AT 1200°C

Compound	$-\log P_{O_2}$ (atm)	Other phases	a (Å)	b (Å)	c (Å)	V (Å^3)	Ref.
CeO_2	0.68		5.406 ± 0.001			158.0 ± 0.1	Present
	0.68	Fe_2O_3	5.408 ± 0.001				Present
	12.50		5.409 ± 0.001			158.2 ± 0.1	Present
			5.4110 ± 0.0005				(5)
			5.4110 ± 0.0003				(9)
Fe_2O_3	0.68		5.034 ± 0.001		13.741 ± 0.001		Present
	0.68	CeO_2	5.034 ± 0.001		13.735 ± 0.002		Present
			5.0317		13.737		(32)
Fe_3O_4	7.00		8.395 ± 0.002				Present
	7.00	CeO_2	8.394 ± 0.001				Present
			8.3963				(33)
$CeFeO_3$	7.80		5.515 ± 0.001	5.570 ± 0.001	7.815 ± 0.001	240.1 ± 0.1	Present
	12.30		5.515 ± 0.002	5.569 ± 0.001	7.817 ± 0.001	240.1 ± 0.1	Present
			5.520	5.539	7.820	239.1	(20)
			5.541	5.577	7.809	241.3	(31)
			5.519	5.536	7.819	238.9	(18)

TABLE IV

THE STANDARD GIBBS ENERGIES OF REACTIONS

Reaction	Temp. (°C)	$-\log P_{O_2}$ (atm)	$-\Delta G°$ (kJ)	$-\Delta G°$[a] (kJ)
(1) $\frac{2}{3}Ce_2O_3 + \frac{1}{4}O_2 = Ce_3O_5$	1153	17.65	120.5	
	1200	16.70	117.7	
	1249	16.00	116.6	
	1310	15.10	114.4	
	1330	14.83	113.8	
(2) $\frac{1}{3}Ce_3O_5 + \frac{1}{8}O_2 = CeO_2$	1153	16.91	61.7	
	1200	16.27	59.6	
	1249	15.55	57.0	
	1310	14.87	55.3	
	1330	14.57	54.5	
(3) $\frac{1}{3}Fe_3O_4 + CeO_2 = CeFeO_3 + \frac{1}{8}O_2$	1000	10.72	−43.3	−41.5
	1100	8.63	−36.3	−37.0
	1200	7.25	−33.7	−32.4
(4) $CeO_2 + Fe + \frac{1}{2}O_2 = CeFeO_3$	1000	15.68	193.5	190.8
	1100	13.96	187.7	183.2
	1200	12.48	181.4	175.6

[a] From Tretyakov *et al.*

and (4), Tretyakov *et al.* have presented general equations, $\log P_{O_2}(\text{atm}) = 14.23 - (31{,}085/T)$ and $\log P_{O_2}(\text{atm}) = 8.02 - (30{,}150/T)$, respectively. $\Delta G°$ values calculated from these equations are also shown in the last column in Table IV. These values are in fairly good agreement with ours.

The standard Gibbs energies of a reaction (5) $\frac{1}{2}Ce_2O_3 + \frac{1}{4}O_2 = CeO_2$, those of a reaction (6) $\frac{1}{2}Ce_2O_3 + Fe + \frac{3}{4}O_2 = CeFeO_3$, and those of a reaction (7) $\frac{1}{2}Ce_2O_3 + \frac{1}{2}Fe_2O_3 = CeFeO_3$ can be calculated from the values of reactions (1) and (2), from those of reactions (4) and (5), and from those of reactions (6) and $2Fe + \frac{3}{2}O_2 = Fe_2O_3$. The relationship between $\Delta G°$ and T was found to be linear. $\Delta G°(1) = -171.4 + 0.0360T$ (±1.0 kJ, 1153–1330°C), $\Delta G°(2) = -119.9 + 0.0403T$ (±1.0 kJ, 1153–1330°C), $\Delta G°(3) = 103.7 - 0.0480T$ (±1.5 kJ, 1000–1200°C), and $\Delta G°(4) = -270.6 + 0.0605T$ (±1.5 kJ, 1000–1200°C) were obtained for the respective reactions by the least-squares method.

References

1. D. J. M. BEVAN, *J. Inorg. Nucl. Chem.* **1,** 49 (1955).
2. G. BRAUER, K. A. GINGERICH, AND U. HOLTZSCHMIDT, *J. Inorg. Nucl. Chem.* **16,** 77 (1960).
3. G. BRAUER AND K. A. GINGERICH, *J. Inorg. Nucl. Chem.* **16,** 87 (1960).
4. F. A. KUZNETSOV, V. I. BELIY, AND T. N. REZUKHINA, *Dokl. Akad. Nauk SSSR, Ser. Fiz. Khim.* **139,** 1405 (1961).
5. D. J. M. BEVAN AND J. KORDIS, *J. Inorg. Nucl. Chem.* **26,** 1509 (1964).
6. J. CAMPSERVEUX AND P. GERDANIAN, *J. Chem. Thermodyn.* **6,** 795 (1974).
7. R. J. PANELNER, R. N. BLUMENTHAL, AND J. E. GARNIER, *J. Phys. Chem. Solid* **36,** 1213 (1975).
8. B. IWASAKI AND T. KATSURA, *Bull. Chem. Soc. Jpn.* **44,** 1297 (1971).
9. O. TOFT SØRENSEN, *J. Solid State Chem.* **18,** 217 (1976).
10. N. KIMIZUKA AND T. KATSURA, *Bull. Chem. Soc. Jpn.* **47,** 1801 (1974).
11. K. KITAYAMA AND T. KATSURA, *Bull. Chem. Soc. Jpn.* **49,** 998 (1976).
12. T. SUGIHARA, N. KIMIZUKA, AND T. KATSURA, *Bull. Chem. Soc. Jpn.* **48,** 1806 (1975).

13. N. KIMIZUKA AND T. KATSURA, *J. Solid State Chem.* **15,** 151 (1975).
14. T. SEKINE AND T. KATSURA, *J. Solid State Chem.* **17,** 49 (1976).
15. T. KATSURA, T. SEKINE, K. KITAYAMA, T. SUGIHARA, AND N. KIMIZUKA, *J. Solid State Chem.* **23,** 43 (1978).
16. T. SUGIHARA, theses, Tokyo Institute of Technology, 1978.
17. N. TANNIERES, theses, L'universite de Nancy I, 1974.
18. F. BERTAUT AND F. FORRAT, *J. Phys. Radium* **17,** 129 (1956).
19. F. BERTAUT AND F. FORRAT, *C.R. Acad. Sci. Paris* **244,** 96 (1957).
20. YU. D. TRETYAKOV, V. V. SOROKIN, A. R. KAUL, AND A. P. ERASTOVA, *J. Solid State Chem.* **18,** 253 (1976).
21. L. S. DARKEN AND R. W. GURRY, *J. Amer. Chem. Soc.* **67,** 1398 (1945).
22. L. S. DARKEN AND R. W. GURRY, *J. Amer. Chem. Soc.* **68,** 798 (1946).
23. T. SMILTENS, *J. Amer. Chem. Soc.* **79,** 4877 (1957).
24. P. E. C. BRYANT AND W. W. SMELTZER, *J. Electrochem. Soc.* **116,** 1409 (1969).
25. R. A. GIDDINGS AND R. S. GORDAN, *J. Amer. Ceram. Soc.* **56,** 111 (1973).
26. N. KIMIZUKA AND T. KATSURA, *J. Solid State Chem.* **13,** 176 (1975).
27. T. KATSURA AND H. HASEGAWA, *Bull. Chem. Soc. Jpn.* **40,** 561 (1967).
28. T. KATSURA AND A. MUAN, *Trans. AIME* **230,** 77 (1964).
29. I. IWASAKI, T. KATSURA, M. YOSHIDA, AND T. TARUTANI, *Jpn. Anal.* **6,** 211 (1957). (in Japanese)
30. J. FABER, JR., M. A. SEITZ, AND M. H. MEULLER, *J. Phys. Chem. Solid* **37,** 903 (1976).
31. M. ROBBINS, G. K. WERTHEIM, A. MENTH, AND R. C. SHERWOOD, *J. Phys. Chem. Solid* **30,** 1823 (1968).
32. JCPDS Card No. 13-534.
33. JCPDS Card No. 11-614.